



## Excited state proton transfer in a ‘super’ photoacid based on a phenol–pyridinium biaryl chromophore

J.-Pierre Malval<sup>a,\*</sup>, Vincent Diemer<sup>b</sup>, Fabrice Morlet Savary<sup>a</sup>, Patrice Jacques<sup>a</sup>, Xavier Allonas<sup>a</sup>,  
Hélène Chaumeil<sup>b</sup>, Albert Defoin<sup>b</sup>, Christiane Carré<sup>c</sup>

<sup>a</sup>Département de Photochimie Générale, UMR CNR 7525, Université de Haute Alsace, ENSCMu 3 rue Alfred Werner, 68093 Mulhouse, France

<sup>b</sup>Laboratoire de Chimie Organique et Bioorganique, UMR CNRS 7015, University of Haute Alsace, ENSCMu 3 rue Alfred Werner, 68093 Mulhouse, France

<sup>c</sup>Foton, CNRS UMR 6082, Département Optique, Technopôle Brest Iroise CS 83818, 29238 Brest Cedex, France

### ARTICLE INFO

#### Article history:

Received 10 August 2007

In final form 19 February 2008

Available online 2 March 2008

### ABSTRACT

We report the effect of a *N*-methylpyridinium substituent on the photoacidity enhancement of a phenol derivative. The steady-state and time-resolved fluorescence of this new phenolic ‘super’ photoacid (HPPy) are measured in different solvents in comparison with its methoxy analogue (MPPy). Solvatochromic shifts and nonradiative rate constants ascribable to excited state proton transfer (ESPT) are correlated with the empirical Kamlet–Taft parameters ( $\pi^*$ ,  $\alpha$ , and  $\beta$ ). Whereas, spectral shift of MPPy is mainly correlated to  $\pi^*$  parameter, HPPy is also strongly influenced by  $\beta$ . At 77 K, ESPT is hampered and leads to the switch ‘on’ emission of conjugated base.

© 2008 Elsevier B.V. All rights reserved.

### 1. Introduction

Photoacid generators (PAG) are attracting systems for high resolution photoresists applied in microelectronics [1]. Acid photo-production can catalyse a sequential deprotection of a polymeric acid-cleavable group which constitutes a decisive step in the chemical amplification process [2]. However, conventional PAGs undergo irreversible photoreactions that can also generate undesired secondary products [3,4]. An alternative solution is the use of transient photoacid generators (TPAG). In this case, acid photo-production and subsequent primary acid-sensitive reaction are only possible during excited state lifetime of TPAG, before reversible relaxation to ground state. This cycling process can enable a better control of resulting chemistry. However, the problem of TPAG utilization is still not solved. Hydroxyarene derivatives exhibit a strong acidity enhancement upon electronic excitation [5,6]. For instance, the  $pK_a$  of 2-naphthol drops of 7 units in  $S_1$  state [7], proton transfer to water is then possible within excited-state lifetime (ca. 8 ns). Moreover, acidity in  $S_1$  state can be increased by aromatic substitution with electron withdrawing group [8,9]. The excited state proton transfer (ESPT) enhancement is commonly explained by an intramolecular charge transfer (ICT) from hydroxyl oxygen to its distal aromatic ring. However, it was shown that the exothermy of ICT is mainly stemmed from excited state properties of the conjugated base ( $R^*O^-$ ) [10]. Granucci et al. have corroborated such an adding effect by ab initio calculations on phenol and cyanophenols [11]. Substituents effect provides therefore a rel-

evant probe for ICT. In a search for stronger photoacids that can act as TPAGs, we report here the photophysical properties of a phenol derivative bearing a pyridinium substituent in *para* position, the 4-(4-(2,6-di-*tert*-butylphenol))*N*-methylpyridinium (HPPy) (Scheme 1). We compare the behavior of HPPy with its methoxy analogue, the 4-(4-(2,6-di-*tert*-butylanisole))*N*-methylpyridinium (MPPy).

### 2. Experimental

#### 2.1. Materials

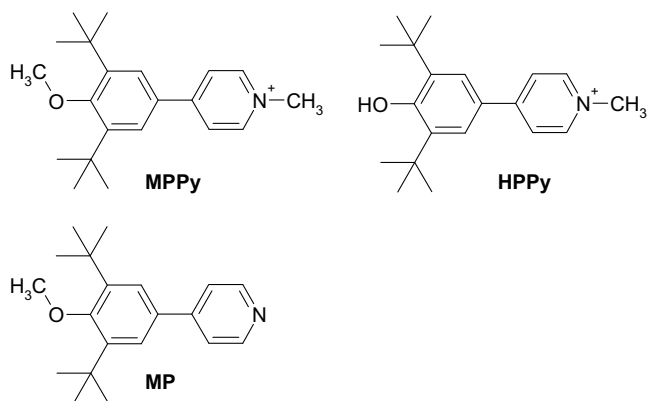
The synthesis of zwitterion form of the HPPy is based on a similar method described in Ref. [12]. The details of synthesis will be described elsewhere. To obtain HPPy from its zwitterion form, a stoichiometric amount of trifluoroacetic acid is added (typically  $3 \times 10^{-6}$  M), the total disappearance of the last absorption band of the zwitterion confirms the quantitative conversion. MPPy and MP are derived from a hydroxyl protected intermediate in this synthesis. In all cases the counterion of the cationic chromophores is  $CF_3COO^-$ . The presence of crowded *tert*-butyl substituents prevent self-aggregation, this was confirmed by checking the linear relationship between absorbance and concentration within mM range. All solvents were Aldrich and Fluka Spectrograde.

#### 2.2. Apparatus and methods

The absorption measurements were carried out with a Perkin Elmer Lambda 2 spectrometer. A FluoroMax 4 Luminescence Spectrometer was used for the fluorescence measurements. The fluorescence spectra were spectrally corrected; the fluorescence

\* Corresponding author.

E-mail address: [jean-pierre.malval@uha.fr](mailto:jean-pierre.malval@uha.fr) (J.-P. Malval).



Scheme 1. Molecular structures of the compounds.

quantum yields (that include the correction due to the solvent refractive index) were determined relatively to quinine bisulfate in 0.05 M sulfuric acid ( $\varphi = 0.52$ ) [13].

The fluorescence lifetimes were measured using a Nano LED emitting at 344 nm as an excitation source with a nano led controller module, Fluorohub from IBH, operating at 1 MHz. The detection was based on a R928P type photomultiplier from Hamamatsu with

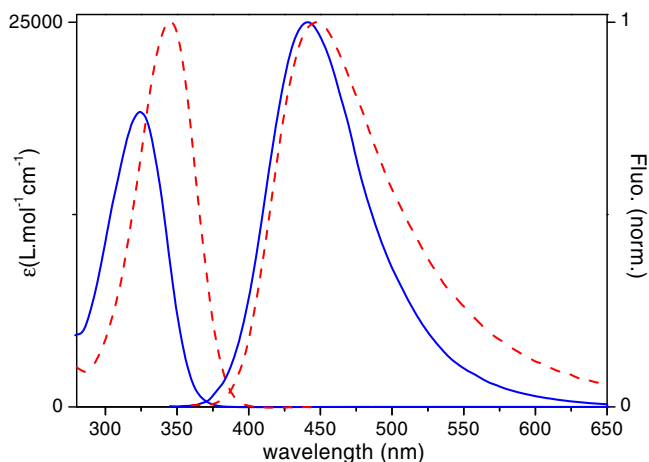


Fig. 1. Absorption and fluorescence spectra of HPPy (dashed lines) and MPPy (full lines) (solvent: acetonitrile).

Table 1  
Photophysical data of HPPy and MPPy

	MPPy				HPPy				
	$\lambda_a$ (nm)	$\lambda_f$ (nm)	$\Phi_f$	$\tau_f$ (ns)	$\lambda_a$ (nm)	$\lambda_f$ (nm)	$\Phi_f$	$\tau_f$ (ns)	$k_{nr}$ $10^9$ s $^{-1}$
BOE <sup>a</sup>	311	399	0.11	–	350	413	0.031	–	–
EOE <sup>a</sup>	310	407	0.11	1.99	348	424	0.016	<0.10	3.0
BuAc <sup>a</sup>	315	417	0.15	1.05	345	425	0.050	0.24	1.9
BuCl <sup>a</sup>	–	421	0.26	–	358	434	–	–	–
THF <sup>a</sup>	316	426	0.30	2.57	353	432	0.011	<0.10	10
CH <sub>2</sub> Cl <sub>2</sub> <sup>a</sup>	336	442	0.35	3.72	374	432	0.47	5.05	–
PPCN <sup>a</sup>	324	442	0.28	1.71	346	446	0.11	1.72	0.9
ACN <sup>a</sup>	325	440	0.11	1.36	345	448	0.11	1.76	–
Acetone	–	438	0.27	1.91	347	440	0.010	–	14
2-Propanol	325	423	0.33	2.01	357	412	0.002	–	82
EtOH <sup>a</sup>	322	428	0.35	2.10	355	409	0.001	<0.10	166
MeOH <sup>a</sup>	320	430	0.27	–	352	410	<0.001	–	–
TFE <sup>a</sup>	335	445	0.18	1.92	360	445	0.14	1.49	0.1

<sup>a</sup> BOE: butyl ether, EOE: ethyl ether, BuAc: butyl acetate, BuCl: butyl chloride, THF: tetrahydrofuran, CH<sub>2</sub>Cl<sub>2</sub>: dichloromethane, PPCN: propionitrile, ACN: acetonitrile, EtOH: ethanol, MeOH: methanol, TFE: trifluoroethanol.

high sensitivity photon-counting mode. The decays were fitted with the iterative reconvolution method on the basis of the Marquardt/Levenberg algorithm [14]. Such a reconvolution technique allows an overall-time resolution down to 0.1 ns. The quality of the exponential fits was checked using the reduced  $\chi^2$  ( $\leq 1.2$ ).

### 3. Results and discussion

Fig. 1 displays absorption and fluorescence spectra of MPPy and HPPy in acetonitrile and Table 1 gathers their corresponding spectroscopic data in 13 solvents. The last absorption band of MPPy and HPPy is located in the 300–380 nm region. This band corresponds to an electronic transition with charge transfer character from the phenol (moderate donor) to pyridinium moiety (strong acceptor). Absorption band of MPPy is blue shifted and less intensive in comparison with its hydroxylic analogue, values of maximum extinction coefficients are  $1.8$  and  $2.5 \times 10^4$  L mol $^{-1}$  cm $^{-1}$ , respectively. While absorption band of MPPy is mainly red shifted when increasing solvent polarity; absorption band of HPPy does not shift monotonously indicating specific solute–solvent interactions at ground state. Such solute–solvent interactions will be further described in the framework of the empirical solvatochromic scale of Kamlet–Taft [15,16]. For MPPy, sterical hindrance around the methoxy group should hamper an optimal conjugation of oxygen atom with its distal aromatic ring, inducing therefore a band blue shift with respect to the absorption of HPPy. Reciprocally, the relative excess red shift of the absorption band of HPPy is better understood as a more pronounced contribution of the quinoid mesomeric form to the S<sub>0</sub>–S<sub>1</sub> electronic transition. Therefore, such a near planar structure leads to a maximum orbital overlap which is consistent to the observed red shift. As a consequence, the phenolic hydrogen lability is also enhanced at the ground state due to the partial positive charge on the oxygen.

Both HPPy and MPPy exhibit an unstructured fluorescence band in 380–560 nm region. In this case, emission bands are clearly red shifted by increasing solvent polarity. If we only take into account the dipole–dipole interaction for the contribution of the solvent to the energy of the excited states (hydroxylic solvents are thus excluded), the dipole moment of the emitting excited state can be evaluated from the Lippert–Mataga equation [17,18]

$$V_{\text{fluo}} = -\frac{2\mu_e(\mu_e - \mu_g)}{hca^3} \cdot \Delta f + C^{\text{te}}$$

where  $\mu_e$  is the excited state dipole moment;  $\mu_g$  is ground state dipole moment calculated from AM1 method [19];  $\Delta f$  is the solvent

polarity parameter defined by  $\Delta f = (\epsilon - 1)(2\epsilon + 1) - 0.5 \cdot (n^2 - 1) / (2n^2 + 1)$ , where  $\epsilon$  is the relative permittivity and  $n$  is the refractive index of the solvent,  $a$  is the Onsager radius, estimated to 5 Å from the calculated spherical solvent shell around the molecule,  $h$  is the Planck constant and  $c$  is the speed of light. We also assume that the dipole moment of the Franck–Condon ground state reached upon emission from the relaxed excited state is identical with the ground state dipole moment  $\mu_g$ . Calculated  $\mu_e$  for HPPy and MPPy are both similar with a value roughly equal to 20 D (Table 2).  $S_1$  states exhibit therefore a significant charge transfer character.

Such a large excited intramolecular charge transfer process can also be correlated to the photophysical effect of the pyridine protonation in MP compound. The 0–0 transition energy is then strongly decreased with a variation of 5950  $\text{cm}^{-1}$ . Applying a Förster cycle [20] to evaluate the change of basicity from the ground state to the excited state, leads to a large  $\text{p}K_a$  increase of 12.4 units. This value should be considered as an estimation since we assume an equivalent entropies of reaction between ground and excited states. However, the trend is clear: consecutive to a light induced excited CT process, nitrogen of the pyridine moiety exhibits a charge density enhancement which strongly favours its basicity.

While the fluorescence quantum yield and fluorescence lifetime of MPPy are weakly affected by solvent nature, a striking contrast is observed for HPPy whose fluorescence is strongly quenched in hydrogen bond accepting solvents (Table 1). Radiative rate constants of MPPy and HPPy have an average value of 1.15 and  $1.04 \times 10^8 \text{ s}^{-1}$ , respectively, it thus confirms the electronic equivalency of the two emitting states. However, in the case of HPPy the presence of the hydroxyl group leads to an adding deactivation pathway with  $k_{nr}$  as rate constant. Such a de-excitation process can be confidently ascribed to H-bond-induced quenching. Using MPPy as model compound, an estimation of the nonradiative rate constant of HPPy ( $k_{nr}$ ) can be derived from the following equation

$$k_{nr} = k_r^0 (1/\Phi - 1/\Phi_0)$$

where  $\Phi$ ,  $\Phi_0$  denote emission quantum yields of HPPy and MPPy in a given solvent,  $k_r^0$  is the radiative rate constant of MPPy. Moreover, the non fluorescence of the conjugated base of HPPy suggests the occurrence of an excited state proton transfer process (ESPT) as a possible deactivation pathway. In this case, the calculation assumes that adiabatic geminate recombination is negligible [9,21]. The profiles of fluorescence lifetime decay of HPPy support such an assumption since they do not exhibit the long time tail that decays as a power law at  $t^{-3/2}$ , fingerprint of a reversible pair kinetics [22]. Table 1 shows  $k_{nr}$  for each solvent. The nonradiative rate constant is strongly solvent dependent, its value fluctuates from  $1.0 \times 10^8 \text{ s}^{-1}$  in trifluoroethanol to  $1.7 \times 10^{11} \text{ s}^{-1}$  ethanol. The latter value indicates a very efficient ultra fast process between excited HPPy and ethanol.

To quantify solute–solvent interactions at the ground state and the excited state, we use Kamlet–Taft solvatochromic parameters [15,16]:  $\pi^*$ ,  $\alpha$  and  $\beta$ . Parameter  $\pi^*$  is a measure of the non-specific solvent polarity/polarizability, whereas  $\alpha$  and  $\beta$  indicate the solvent hydrogen bond (HB) donating and accepting properties. The spectral shift can therefore be linearly correlated with these parameters by

$$\nu_{\text{fluor}} = \nu_0 + p\pi^* + a\alpha + b\beta$$

**Table 2**  
Ground and excited-state dipole moments of HPPy and MPPy

	$m^a$ ( $\text{cm}^{-1}$ )	$\mu_g^b$ (D)	$\mu_e$ (D)
MPPy	–12 500	10.8	19.0
HPPy	–9 500	10.5	17.3

<sup>a</sup> Solvatochromic slopes of fluorescence.

<sup>b</sup> From AM1 calculation.

**Table 3**  
Kamlet–Taft coefficients of compounds

	$S_0$				$S_1$			
	$p$ ( $\text{cm}^{-1}$ )	$a$ ( $\text{cm}^{-1}$ )	$b$ ( $\text{cm}^{-1}$ )	$R$	$p$ ( $\text{cm}^{-1}$ )	$a$ ( $\text{cm}^{-1}$ )	$b$ ( $\text{cm}^{-1}$ )	$R$
MPPy	–2750	–100	–700	0.877	–4100	–40	120	0.967
HPPy	120	130	–2820	0.976	–3140	860	2340	0.954

Coefficients  $p$ ,  $a$  and  $b$  are related to solute properties:  $p$  refers to solute dipole moment,  $a$  evaluates its ability to donate a HB to solvent,  $b$  measures the tendency of the solute to accept a HB from the solvent. Excluding haloaliphatic solvents which deviate from correlation, multi-linear regressions to the absorption and emission data lead to coefficients listed in Table 3.

Solvent induced spectral shift on the absorption and emission of MPPy is mainly correlated to  $\pi^*$  parameter whose coefficient accounts 80% and 95% of the spectral shift, respectively. Besides, the stronger red shift measured for  $S_1$  state is consistent with the larger dipole moment measured at  $S_1$  state.

However for HPPy the analysis is markedly different. In the ground state, solvent induced spectral shift is mainly governed by  $\beta$  parameter. The hydrogen bond acceptance of the solvent promotes the lability of the hydroxylic hydrogen of HPPy. As a consequence, the electronic contribution of quinoid resonant form increases in the  $S_0$ – $S_1$  transition which leads to a more pronounced red shift of the last absorption band in comparison with MPPy. At the excited state, HPPy both exhibits a strong dependency to  $\pi^*$  and  $\beta$  parameters. While  $b$  coefficient displays a negative value at  $S_0$  state, it is unusually positive for  $S_1$  one and roughly accounts 40% of the spectral shift. This suggests that the energy level of the emitting excited species raises by increasing solvent basicity. It constitutes an atypical converse effect as those observed for 2-naphthol [8,23] or pyranine [24] derivatives. However, in our case, the photophysical dynamics at  $S_1$  state is somewhat different. Actually, the large Stokes-shift observed for HPPy indicates an emitting geometry and/or electronic configuration different from the absorbing one. Further, the ratio between radiative rate constant of HPPy in acetonitrile and its calculated Strickler–Berg [25] rate constant has a value of 0.3 which strongly deviates from unity. Therefore, a geometric relaxation as intramolecular twisting between the two phenyl rings should occur at  $S_1$  state and lead to a less planar structure as opposed to the ground state. Recent low-temperature measurements and ab initio calculations [26] clearly demonstrated that anilinyridinium derivatives undergo an energetic barrierless twist relaxation towards 90° energetic minimum at  $S_1$  state. From picosecond time-resolved fluorescence measurements, Fromherz et al. [27] rationalize this conformational change by a two-state model of rotamerism. Two emitting rotamers are in very fast equilibration at the excited state: the first rotamer exhibits a near planar conformation and emits in the blue part of the fluorescence spectrum whereas the second one with a more twisted conformation emits in the red region. Assuming a complete transposition of this precursor–successor model to HPPy, the hypsochromy emission shift with increasing solvent basicity can be explained by a more efficient nonradiative deactivation of the twisted geometry than the planar one. The relative population of the blue emitting rotamers should consequently increase.

Interestingly the efficiency of the nonradiative process is also influenced by the solvent basicity. A good correlation is indeed obtained between  $k_{nr}$  in logarithmic scale and  $\beta$  parameter (Fig. 2) which confirms the quenching efficiency of ESPT. The exothermy of the overall dissociation is largely determined by proton solvation dynamic along hydrogen bond which connects the proton donor (solute) and the proton acceptor (solvent).

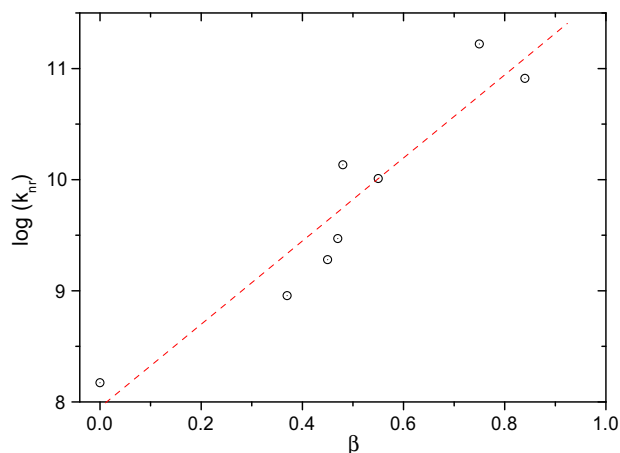


Fig. 2. Dependence of the nonradiative rate constants on the basicity parameter  $\beta$ .

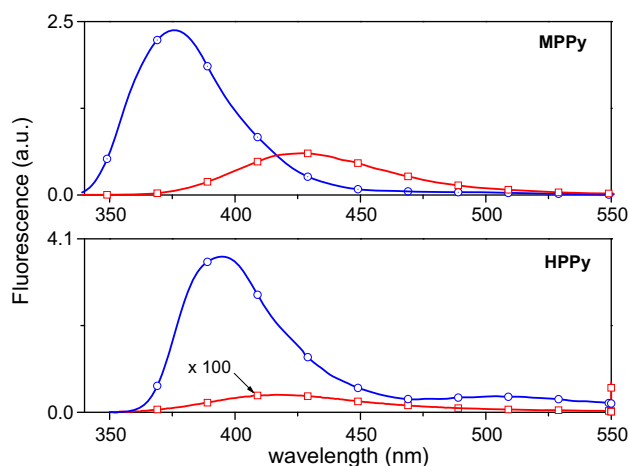


Fig. 3. Fluorescence spectra of MPPy and HPPy in ethanol at room temperature (squares) and 77 K (circles).

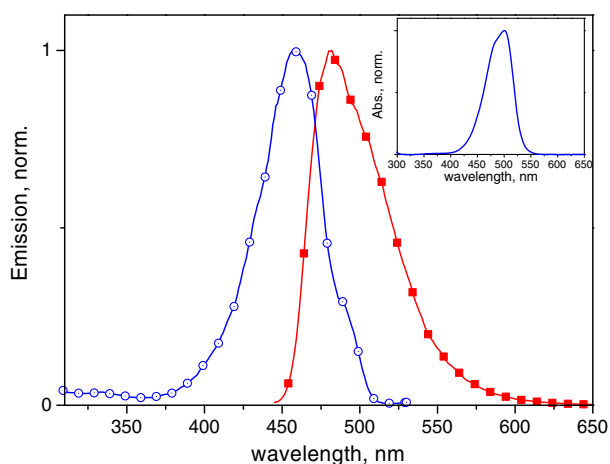


Fig. 4. Emission (squares) and excitation (circles) spectra of HPPy in basic solution of ethanol at 77 K. Inset: Absorption spectrum at room temperature of conjugated base of HPPy.

At very low temperature, radiationless processes are mainly suppressed, Fig. 3 shows fluorescence spectra of compounds at

room temperature, and at 77 K in ethanol. Fluorescence emission of HPPy and MPPy are blue shifted and strongly enhanced. This enhancement is 100 times higher for HPPy than for MPPy. Furthermore emission of HPPy exhibits a new band at 490 nm with a corresponding fluorescence lifetime of 3.2 ns. Fig. 4 shows excitation and emission spectra of phenolate conjugated base of HPPy in glassy matrix of ethanol, its emission lifetime is also 3.3 ns. Therefore, the observed red-emission band can be confidently attributed to phenolate excited species. This finally indicates that ESPT is a strongly allowed process which is not totally suppressed at low temperature.

#### 4. Conclusion

Excited state proton transfer in HPPy was investigated in comparison with its methoxy analogue. Anomalous red shift observed for the absorption of the 'super' photoacid was attributed to a more pronounced electronic contribution of the quinoid mesomeric structure. As a consequence the lability of the hydroxylic hydrogen is enhanced at ground state. At  $S_1$  state, a fast equilibrium between a planar and a twisted rotamer distribution occurs. The increase of solvent  $\beta$  parameter promotes a preferential quenching of the twisted geometry. Furthermore, nonradiative deactivation process is mainly dependent to hydrogen bond solvent acceptancy,  $k_{nr}$  is 1600 times higher in ethanol than in TFE. Therefore, ESPT appears as a main quenching pathway. This photoinduced proton transfer leads a non-emissive excited phenolate [28]. At 77 K, the switch 'on' emission of phenolate indicates the occurrence of ESPT even at low temperature.

#### References

- [1] H. Ito, C.G. Willson, *Polymers in Electronics*, in: T. Davidson (Ed.), ACS Symposium Series 242, ACS, Washington, DC, 1984.
- [2] S.P. Pappas, *J. Imaging Technol.* 11 (1985) 146.
- [3] J.-P. Malval, F. Morlet-Savary, X. Allonas, J.-P. Fouassier, S. Suzuki, S. Takahara, T. Yamaoka, *Chem. Phys. Lett.* 443 (2007) 323.
- [4] J. Andraos, G.G. Barclay, D.R. Medeiros, M.V. Baldovi, J.C. Scaiano, R. Sinta, *Chem. Mater.* 10 (1998) 1694.
- [5] P. Wan, D. Shukla, *Chem. Rev.* 93 (1993) 571.
- [6] S.G. Schulman, W.R. Vincent, W.J.M. Underberg, *J. Phys. Chem.* 85 (1981) 4068.
- [7] A. Weller, *Prog. React. Kinet.* 1 (1961) 187.
- [8] K.M. Solntsev, D. Huppert, N. Agmon, *J. Phys. Chem. A* 103 (1999) 6984.
- [9] L.M. Tolbert, K.M. Solntsev, *Acc. Chem. Res.* 35 (2002) 19.
- [10] N. Agmon, W. Rettig, C. Groth, *J. Am. Chem. Soc.* 124 (2002) 1089.
- [11] G. Granucci, J.T. Hynes, P. Millié, T.-H. Tran-Thi, *J. Am. Chem. Soc.* 122 (2000) 12243.
- [12] V. Diemeil, H. Chaumeil, A. Defoin, A. Fort, A. Boeglin, C. Carré, *Eur. J. Org. Chem.* (2006) 2727.
- [13] R. Meech, D. Phillips, *J. Photochem.* 23 (1983) 193.
- [14] D.V. Connor, D. Phillips, *Time Correlated Single Photon Counting*, Academic Press, London, 1984.
- [15] M.J. Kamlet, J.L.M. Abboud, M.H. Abraham, R.W. Taft, *J. Org. Chem.* 48 (1983) 2877.
- [16] C. Laurence, P. Nicolet, M.T. Dalati, J.-L.M. Abboud, R. Notario, *J. Phys. Chem.* 98 (1994) 5807.
- [17] W. Lippert, *Angew. Chem. Int. Ed. Engl.* 8 (1969) 177.
- [18] N. Mataga, Y. Kaifu, M. Koizumi, *Bull. Chem. Soc. Jpn.* 29 (1956) 465.
- [19] HYPERCHEM, v. 7.03, Hypercube, Inc., Gainesville, FL, 2002.
- [20] T. Förster, *Z. Elektrochem.* 54 (1950) 42.
- [21] D. Huppert, L.M. Tolbert, S. Linares-Samaniego, *J. Phys. Chem. A* 101 (1997) 4602.
- [22] D. Pines, E. Pines, *J. Chem. Phys.* 115 (2001) 951.
- [23] K.M. Solntsev, D. Huppert, L.M. Tolbert, N. Agmon, *J. Am. Chem. Soc.* 120 (1998) 7981.
- [24] J.T. Hynes, T.-H. Tran-Thi, G. Granucci, *J. Photochem. Photobiol., A: Chem.* 154 (2002) 3.
- [25] S.J. Strickler, R.A. Berg, *J. Chem. Phys.* 37 (1962) 814.
- [26] V. Kharlanov, W. Rettig, *Chem. Phys.* 332 (2007) 17.
- [27] C. Röcker, A. Heilemann, P. Fromherz, *J. Phys. Chem.* 100 (1996) 12172.
- [28] A.L. Sobolewski, W. Domcke, *J. Phys. Chem. A* 111 (2007) 11725.